DEUTSCHES ELEKTRONEN-SYNCHROTRON DESY

DESY SR 84-11
April 1984

PHOTOCONDUCTION IN RARE GAS FLUIDS DOPED BY SMALL ORGANIC MOLECULES

by

R. Reininger, V. Saile

Hamburger Synchrotronstrahlungslabor HASYLAB at DESY

P. Laporte

Equipe de Spectroscopie C.N.R.S. (LA 171), Saint Etienne

I.T. Steinberger

Racah Inst. of Physics, The Hebrew University, Jerusalem

ISSN 0723-7979

NOTKESTRASSE 85 · 2 HAMBURG 52

To be sure that your preprints are promptly included in the
HIGH ENERGY PHYSICS INDEX ,
send them to the following address (if possible by air mail) :

DESY
Bibliothek
Notkestrasse 85
2 Hamburg 52
Germany

DESY SR 84-11
April 1984

ISSN 0723-7979

Photoconduction in rare gas fluids doped by small organic molecules

R. Reininger[a], V. Saile[a], P. Laporte[b] and I.T. Steinberger[c]

a HASYLAB, Deutsches Elektronen-Synchrotron DESY, Notkestr. 85, 2000 Hamburg 52, Germany

b Equipe de Spectroscopie C.N.R.S. (LA 171), 158 bis cours Fauriel, 42023 Saint Etienne Cedex, France

c Racah Institute of Physics, The Hebrew University, Jerusalem, Israel

Abstract

Impurity photoconduction was studied in fluid argon, krypton and xenon doped by one of the impurities ethane, propane, butane and benzene. For several impurity:host combinations it was possible to determine, in a wide density range, the energy needed to raise an electron from the ground state of the impurity to the conduction level of the host. The polarization energy P_+^i of the hole trapped at the impurity was calculated from these results and compared with the Born charging energy formula.

submitted to Chem. Phys.

ISSN 0723 - 7979

1. Introduction

The first report on impurity photoconduction in rare-gas fluids and solids was published recently in this Journal [1]. It presented photoconductivity excitation spectra of fluid argon and krypton, doped by xenon impurity. The spectra reported were obtained by using monochromated synchrotron radiation from the DORIS storage ring at DESY, Hamburg. The samples were enclosed in a cell having a LiF front window and their impurity concentration varied from about two to two hundred p.p.m. The photon energy threshold for photoconduction E_{pc} was identified as the minimum energy E_G^i needed to raise an electron from the ground state of the impurity to the lowest conduction level ("bottom of the conduction band"), or, in short, the internal ionization energy of the impurity in the medium. With these results it was possible to revise the only values of E_G^i hitherto available, namely those obtained from indirect spectroscopic evidence [2]. Moreover, combining E_G^i values from photoconductivity excitation spectra with spectroscopic data [3] assignments of bound excitons and of their binding energies could be revised. Using experimentally determined results [4,5] on the energy V_0 of the quasi-free electrons the polarization energy P_+^i of the hole trapped at the impurity after ionization was also determined. The density range of the experiments on the Xe:Ar and Xe:Kr systems [1] was rather limited since if a host exciton band (or a broadened atomic absorption line) overlaps the threshold region then absorption to the exciton band competes very effectively for the incident photons, diminishing the photocurrent and totally obscuring the threshold. In Xe:Ar and Xe:Kr such overlaps occur for a wide range of densities.

In this paper photoconductivity excitation spectra are presented for argon, krypton and xenon doped by one of the molecular impurities ethane (C_2H_4), propane (C_3H_8), butane (C_4H_{10}) and benzene (C_6H_6). For several impurity:host combinations it proved to be feasible recording such spectra without interference from the host excitons, at host densities ranging from that of a dilute gas to the triple point density ρ_{TP}. Accordingly the variation of E_G^i and P_+^i could be followed in this very wide range, for the first time in any doped fluid. The effects of changing the impurity in a given host could be clearly perceived as well as the effects of the same impurity in different host fluids. Results on E_G^i in the fluids were compared with similar data in the corresponding solids, based on spectroscopic experiments. Finally it was possible to test the applicability of the Born charging energy formula to the dependence of P_+^i on the density for the whole density range in the doped fluids investigated.

2. Experimental results

The experiments were performed as described in Ref. [1]. The only additional problem was the increased danger of freezing out of the impurity, since for some of the systems the difference between the triple points of the host and the impurity was very large. In the extreme case, namely for benzene in argon, the benzene impurity did indeed freeze out at low temperatures, corresponding to densities above 2×10^{22} atoms/cm^3. Measurements in a wide density range were recorded for argon doped by ethane, propane or butane, as well as for benzene impurity in the hosts argon and krypton. Because of host exciton-photoconduction threshold overlap problems (see above) the benzene:xenon system could be studied only at densities near the triple point, for butane:krypton only one useful spectrum was recorded and other combinations of the above listed impurities and hosts could not be investigated at all. Figure 1 shows a typical set of photoconductivity excitation spectra. The system presented is ethane:argon, the parameter changing from graph to graph being the host density. The tendency of the threshold photon energy to decrease with increasing density is evident. The sharp drop on the high-energy sides of the curves is due to the n=1 ($^3P_1$) exciton in fluid argon; this exciton shifts towards the blue with increasing density [6]. The height of the curves is influenced by the shifts of the onset and of the exciton position and also by the variation of the mobility with density [7]: the zero-field mobility has a maximum at a density of 1.21×10^{22} cm^{-3} and a broad minimum at around 0.6×10^{22} cm^{-3}. It should be mentioned here that the overall shape of photoconductivity excitation spectra was sensitive to traces of other dopants as well: the absorption lines of the further impurity appear as dips on the background of the photocurrent continuum determined by the main impurity and the host.

Empirical formulae of the form

$$I \propto (h\nu - E_G)^n \qquad \ldots 1$$

have been suggested in the literature to represent the dependence of the photocurrent I (normalized to equal numbers of absorbed photons) on the photon energy $h\nu$ near the threshold E_G in non-polar liquids [8-11]. The exponent has been usually given some value between 0.5 and 2, but no single value of n was found that would give a good representation for all liquids investigated. In the present work two methods were employed [1] to determine the impurity photoconduction thresholds: a.) noting the photon energy at

the beginning of the rise; for this, the spectra had to be plotted on such scales that they should be roughly congruent in the region in the threshold region (apart from a shift on the photon energy scale); b.) plotting the square root of the photocurrent and extrapolating the linear part of the plot near the threshold until its intercept on the wavelength axis. The second method gave in several cases ambiguous results, namely when two linear regions, with different slopes, appeared on the $\sqrt{I}$ vs. wavelength plots near the threshold or when this plot had a large part with gradually increasing slope in the same region. For any given set of spectra E_G^i was determined by both methods. When the resulting two E_G^i vs. ρ curves were plotted, the two graphs were in each case very similar; they never deviated from each other by more than 0.08 eV and in most cases they were appreciably closer. All data presented below (Figs. 2-5) are based on averages taken from threshold determinations by both methods.

Because of its importance in obtaining correct values of P_+^i (see below), special care was taken when determining the ionization potential I_G^i of the pure dopant. At least four room-temperature spectra were taken for each dopant at a pressure of 260 Pa (≈ 2 torr). For each spectrum, the onset of the photoionzation current was determined by both methods ("initial rise" and "square root") used for finding E_G^i in doped systems. I_G^i-values thus determined should be equal in principle to adiabatic ionization potentials of the pure dopant. Properly averaged I_G^i-s are presented in Table 1, along with first (vertical) ionization potentials from Kimura et al. [12]. It was felt that these I_G^i-values would be more consistent with our E_G^i-values than adiabatic ionization potentials taken from the literature: problems of experimental methods different from ours (e.g., photoelectron spectroscopy, mass spectrometry) and alternative definitions of I_G^i are now avoided. It should be noted that for the case of xenon dopant [1] such a consistent determination of I_G^i was not possible: in this case there is a pronounced photoionization response below the atomic ionization limit, namely at and around higher atomic absorption lines. This is due to the formation of Xe_2^+ dimer ions [13-15].

Figure 2 represents the dependence of the photoconductivity threshold E_G^i on the host density in argon doped by ethane, propane or butane. The impurity concentration was in all cases about 2 ppm. The ionization potentials I_G^i of the impurities are also marked. It is seen that E_G^i is roughly constant at the highest densities, increasing more and more steeply towards I_G^i with decreasing density. The continuous lines drawn are least-squares fittings of quadratic functions to the experimental points.

Figure 3 is similar to Figure 2, but in this case the dopant is identical (benzene) for the three graphs and the hosts are different: argon, krypton or xenon. The density range for the benzene:xenon system was rather narrow because of the proximity of the n=1 ($^3P_1$) host exciton to the photoconductivity threshold. In this system a further photoresponse band also appeared at densities from 0.5 to 1 x 10^{22} cm^{-3} on the low-energy side of the C_6H_6:Xe response; the origin of this band is not understood. For argon and krypton the behaviour of E_G^i vs. ρ at the lowest densities is given as an insert in the graph.

The polarization energy P_+^i of the hole trapped at the impurity was calculated from the relationship [16]

$$E_G^i = I_G^i + V_o + P_+^i \qquad \ldots 2$$

I_G^i being the adiabatic polarization energy of the free impurity molecule. V_o had been determined directly for the host materials employed in this work [4,5]; P_+^i as a function of ρ for argon host and different impurities appears in Figure 4. Since the values of $|P_+^i|$ are rather small compared with I_G^i and E_G^i, and P_+^i is obtained from the algebraic sum of three experimental quantities, particular care was taken to draw the proper error bars in the figure. With these error bars it seems at first sight that the systematic differences between the results for the three dopants are insignificant. However, the two main contributions to the error (both about equally important) come from the determination of I_G^i for the impurity and that of V_o of the host. Now V_o is the same for the three graphs, since they all refer to the host argon: hence it follows that for comparisons between the graphs the error bars should be roughly halved. These shortened error bars would be comparable to the relative displacements of the three graphs in Fig. 4, making the reality of the displacement plausible.

A similar set of P_+^i vs. ρ graphs is shown in Figure 5. They all refer to the same dopant, namely benzene, with different hosts - argon, krypton or xenon. The general shapes of the graphs are similar to those in Figure 4, but there are clear differences between the results for different hosts, $|P_+^i|$ increasing markedly with increasing atomic number. Note that for comparisons of different graphs in this figure the error bar shown should be again roughly halved, since in this case the I_G^i-values are all identical, namely that pertaining to benzene impurity.

3. Discussion

It was pointed out by Messing and Jortner [17] that P_+^i should consist in principle of a sum of a.) an electrostatic contribution and b.) a sum of terms representing short-range repulsive interactions, due to the changes upon ionization between Coulomb, exchange and overlap contributions. They suggested that for an impurity containing many electrons contribution "b" should be considerably smaller than contribution "a". In such an approximation one might expect that with increasing atomic number and atomic polarizability of the host the polarization energy P_+^i should increase in absolute value, while increasing the size of the impurity molecule should cause some decrease in $|P_+^i|$. This latter effect would be due to an increase of the distance between the geometrical centre of the impurity molecule and the surrounding atoms, though the specific location of the positive hole (i.e. its wave function) within the "cavity" defined by the molecule could modify substantially this effect (note also contribution "b" considered above).

It has been shown (Fig. 5) that $|P_+^i|$ increases markedly with increasing atomic number of the host; this indicates the effect of increasing atomic polarizabilities. On the other hand, in Fig. 4 $|P_+^i|$ seems to decrease slightly with increasing size of the molecular impurity; such an effect could be caused by a smaller electrostatic interaction with the host if the positive charge is located in a larger cavity. For further discussions of the P_+^i vs. ρ curves comparison with theory is in order. Messing and Jortner showed [17] that using the Born charging energy formula ([18], see below) in the case of argon host containing xenon impurity gives P_+^i within 10 % of such values as calculated by taking into account the screened electron-atom electrostatic interaction potential, the solute-solvent pair correlation functions and approximating the three-body correlation function by means of the Kirkwood superposition approximation.

Writing the Born charging energy formula as

$$P_+^i = -\frac{e^2}{2\sigma}\left(1 - \frac{1}{\varepsilon_{op}}\right) \qquad \ldots 3$$

ε_{op} being the (optical) dielectric constant, σ has been interpreted [17] as a hard-core diameter determined by both the solute and the solvent. Applications of this formula appear in Figures 4 and 5: in fact the drawn lines are representations of Eq. 3. For the drawings, ε_{op} at the triple-point

densities of the host liquids was taken from Sinnock's work [19] and for other densities it was calculated using the Clausius-Mossotti relation. In Fig. 4, no attempt was made to fit separately each graph obtained for a given impurity. Two values of σ (0.35 and 0.28 nm) were chosen instead, delimiting roughly the possible range of variation of σ for the respective graphs. On the other hand in Fig. 5 an appropriate value of σ was chosen for each graph. We point out that there are some deviations from Eq. 3 that seem to be significant at low densities (see, e.g. C_6H_6:Kr in Fig. 5). Assuming a variation of σ with density by relating it to the Wigner-Seitz radius [17] would worsen the fit between theory and experiment. It should be noted that in Figure 5 the value ofσ seems to vary somewhat erratically with the nature of the host. However, considering the rather large errors in P_+^i the accuracy in the determination of σ cannot be expected to be better than $\pm$ 0.05 nm, thus the above variations do not seem to be significant.

A comparison between the results of argon doped by benzene on one hand and by the alkanes on the other (especially propane) is also of interest. First, for C_6H_6:Ar E_G^i converges very closely (with a slight overshoot) to the value of I_G^i of benzene, while for C_3H_8:Ar its limiting value is definitely lower than I_G^i of propane. As a result of this (note that V_0 is the same in both cases) $|P_+^i|$ for C_6H_6:Ar is markedly smaller (and σ higher) than for the other three doped argon systems. It seems that this situation has to be attributed entirely to slightly different physical meanings of the measured I_G^i for the various materials: variations in the shape of the low-photon energy wing of the photoionization spectrum (because of autoionization, collisional ionization and similar effects) might explain the differences mentioned. A detailed study of the photoionization and photoconduction of the pure dopants as a function of the density and the temperature, coupled with optical absorption measurements, could help to reach more definite conclusions of this point.

Table 2 summarizes some of the experimental results from this work along with comparisons with relevant data from the literature whenever these are available. E_G^i in the liquids near the triple point is compared with E_G^i results obtained by extrapolating Wannier excitonic series observed in the corresponding doped solids (between 10 and 30 K) to $n = \infty$ [20]. It is seen that in the cases such measurements in the solid were, indeed, performed E_G^i in the solid is somewhat larger. The internal consistency of the results

on P_+^i can be checked, on the basis of Table 1, by taking the ratio P_+^i(Kr)/P_+^i(Ar) for benzene impurity and then for butane impurity. In the first case the ratio is 1.6, in the second 1.5. In view of the estimated experimental error this correspondence is rather good. The values of the hard-core diameters in Table 2 are estimates to obtain rough fits in Figs. 4 and 5 and not necessarily equal to the values taken to draw the curves in the figures. It is seen that generally $\sigma < d_0$ of the host solid; the apparent exception of benzene:argon could be attributed to the large error ($\pm$ 0.05 nm) in σ. On the other hand, σ can be either smaller or larger than the characteristic molecular dimension given in the table, though it should be borne in mind that the propane and butane molecules are probably folded at least to some extent when incorporated in the solid or in the dense liquid.

It has been demonstrated above that by combining impurity photoconduction spectra with direct determinations of the energy of the free electron one can obtain consistent values of P_i^+ in wide density ranges. The simple Born charging energy formula proved to be a reasonably good representation of the density-dependence of the polarization energy of the trapped hole in the systems considered. This means that, as expected, the density-dependence of ε_{op} is the main factor in determining the shape of the $P_+^i(\rho)$ curve. However, this simple theory is not adequate on two counts: a.) There are significant deviations from the theoretical predictions, especially at low densities; b.) The value of σ has to be taken as adjustable parameter for each impurity: host combination, with no simple relationship either to the interatomic distance in the host or to the size of the impurity.

On the basis of the results presented it seems that there are good chances to observe impurity photoconduction in rare-gas fluids and in non-polar fluids of small highly symmetric molecules, like, e.g. methane, doped by various molecular impurities. Considering the close relationship of P_+^i with the polarization contribution to the valence-band energy [16,24], such studies should be relevant to the problem of the evolution of electronic energy bands in fluids [25].

References

1 R. Reininger, S. Bernstorff, P. Laporte, V. Saile and I.T. Steinberger, Chem. Phys., in press.

2 G. Baldini, Phys. Rev. 137 (1965) 508.

3 I. Messing, B. Raz and J. Jortner, Chem. Phys. 23 (1977) 23.

4 R. Reininger, U. Asaf and I.T. Steinberger, Chem. Phys. Lett. 90 (1982) 287.

5 R. Reininger, U. Asaf, I.T. Steinberger and S. Basak, Phys. Rev. B28, (1983) 4426.

6 S. Bernstorff, P. Laporte, R. Reininger, V. Saile, I.T. Steinberger and J.L. Subtil, Annals of the Israel Phys. Soc. 6 (1983) 270.

7 S.S.S. Huang and G.R. Freeman, Phys. Rev. A24 (1981) 714.

8 W.F. Schmidt, W. Döldissen, U. Hahn and E.E. Koch, Z. Naturforsch. A33 (1978) 1393.

9 J. Casanovas, R. Grob, D. Delacroix, J.P. Guelfucci and D. Blanc, J. Chem. Phys. 75 (1981) 4661.

10 E.H. Böttcher and W.F. Schmidt, Annals of the Israel Phys. Soc. 6 (1983) 276.

11 E.H. Böttcher and W.F. Schmidt, J. Chem. Phys. 80 (1984) 1353.

12 K. Kimura, S. Katsumatra, Y. Achiba, T. Yamazaki and S. Iwata, Handbook of HeI photoelectron spectra of fundamental organic molecules, Japan Scientific Societies Press, Tokyo, and Halsted Press, New York, 1981.

13 J.A. Hornbeck and J.P. Molnar, Phys. Rev. 84 (1951) 621.

14 R.E. Huffman and D.H. Katayama, J. Chem. Phys. 45 (1966) 138.

15 P. Laporte, V. Saile, R. Reininger, U. Asaf and I.T. Steinberger, Phys. Rev. A28 (1983) 3613.

16 B. Raz and J. Jortner, Chem. Phys. Lett. 4 (1969) 155.

17 I. Messing and J. Jortner, Chem. Phys. 24 (1971) 183.

18 R.A. Holroyd, J. Chem. Phys. 57 (1972) 3007.

19 A.C. Sinnock, J. Phys. C13 (1980) 2375.

20 J. Jortner, in Vacuum Ultraviolet Radiation Physics, ed. E.E. Koch, R. Haensel and C. Kunz (Pergamon-Vieweg, London/Braunschweig, 1974) p. 263.

21 O.G. Peterson, D.N. Batchelder and R.O. Simmons, Phys. Rev. 150 (1966) 703.

22 D.L. Losee and R.O. Simmons, Phys. Rev. 172 (1968) 944.

23 D.R. Sears and H.P. Klug, J. Chem. Phys. 37 (1962) 3002.

24 B. Raz and J. Jortner, Chem. Phys. Lett. 9 (1971) 222.

25 R. Reininger, U. Asaf, I.T. Steinberger, V. Saile and P. Laporte, Phys. Rev. B28 (1983) 3193.

Table 1

I_G^i-values determined in this work (adiabatic, see text) compared with first ionization potentials (vertical, Ref. [12]) for the dopants. All values in eV.

	Ethane	Propane	Butane	Benzene
I_G^i	11.49 ± 0.04	11.02 ± 0.04	10.58 ± 0.09	9.13 ± 0.03
First vertical ionization potental	11.99	11.51	11.09	9.25

Table 2

Ionization potentials E_G^i and polarization energies P_+^i of various molecular impurities in liquid rare-gas hosts near the triple point. The effective hard core diameters σ (see text) nearest-neighbour distances d_o in the host material (solid, near the triple point) and typical molecular dimensions a_m of the impurity are also listed.

	E_G^i (eV) (a)	E_G^i (eV) (b)	P_+^i (eV) (a)	σ(nm) (a)	d_o (nm)	a_m (nm)
C_2H_6:Ar	10.51		-0.78	0.28	0.3865 (c)	0.154 (f)
C_3H_8:Ar	10.03		-0.80	0.29	0.3865 (c)	0.308 (g)
C_4H_{10}:Ar	9.73		-0.64	0.35	0.3865 (c)	0.462 (h)
C_6H_6:Ar	8.38	8.51	-0.56	0.42	0.3865 (c)	0.267 (i)
C_4H_{10}:Kr	9.2		-0.97	0.30	0.4125 (d)	0.462 (h)
C_6H_6:Kr	7.85	8.18	-0.90	0.32	0.4125 (d)	0.267 (i)
C_6H_6:Xe	7.48	7.75	-0.98	0.35	0.4491 (e)	0.267 (i)

(a) Present work
(b) Ref. [20] from spectoscopic data
(c) Ref. [21]
(d) Ref. [22]
(e) Ref. [23]
(f) C-C bond length in alkanes
(g) As (f), times two
(h) As (f), times three
(i) C-C bond length in benzene, times two

Figure Captions

Figure 1 Photoconductivity excitation spectrum of ethane impurity in fluid argon for various densities: a - 0.52, b - 0.75, c - 1.38, d - 1.73 and e - 2.0 x 10^{22} atoms/cm^3. 400 V applied between two electrodes 2 mm apart.

Figure 2 Ionization potentials E_G^i of various impurities in fluid argon as a function of density. ▼ - ethane, ▽ - propane, × - butane.

Figure 3 Ionization potentials E_G^i of benzene impurity in various rare gas hosts as a function of density. ● - argon, × - krypton, * - xenon.

Figure 4 Polarization energy P_+^i of a hole trapped at various impurities in fluid argon as a function of density. ▼ - ethane, ▽ - propane, × - butane.

Figure 5 Polarization energy P_+^i of a hole trapped at a benzene impurity in various rare gas hosts as a function of density. ● - argon, × - krypton, * - xenon.

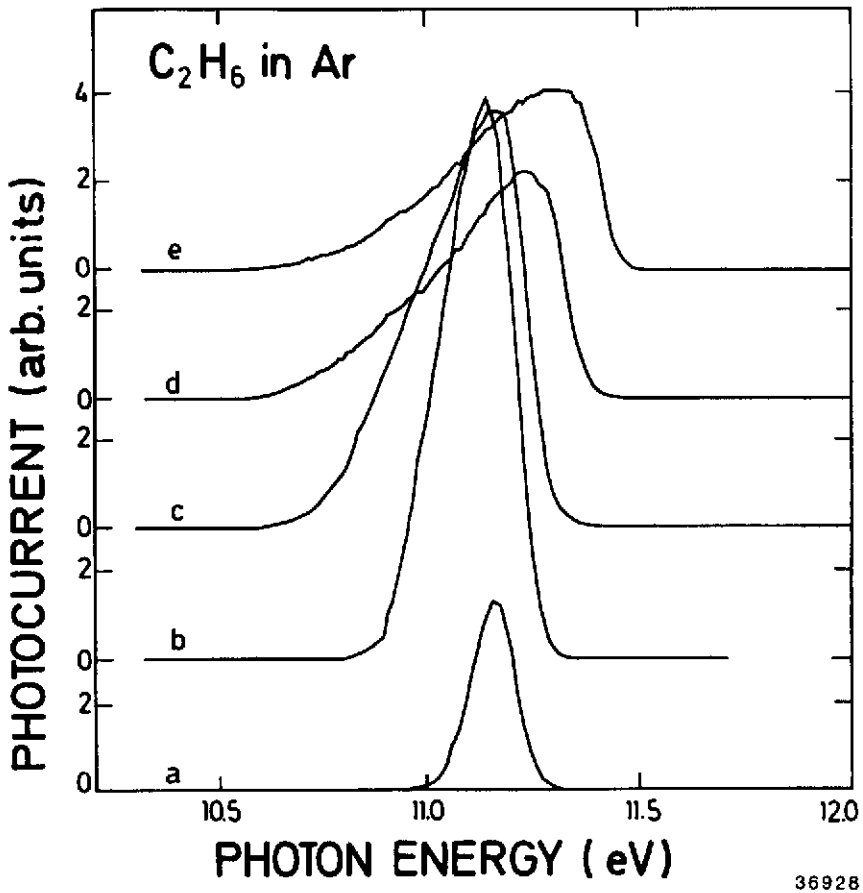
C2H6 in Ar
PHOTOCURRENT (arb. units)
PHOTON ENERGY (eV)
10.5
11.0
11.5
12.0
a
b
c
d
e
36928

Fig. 1

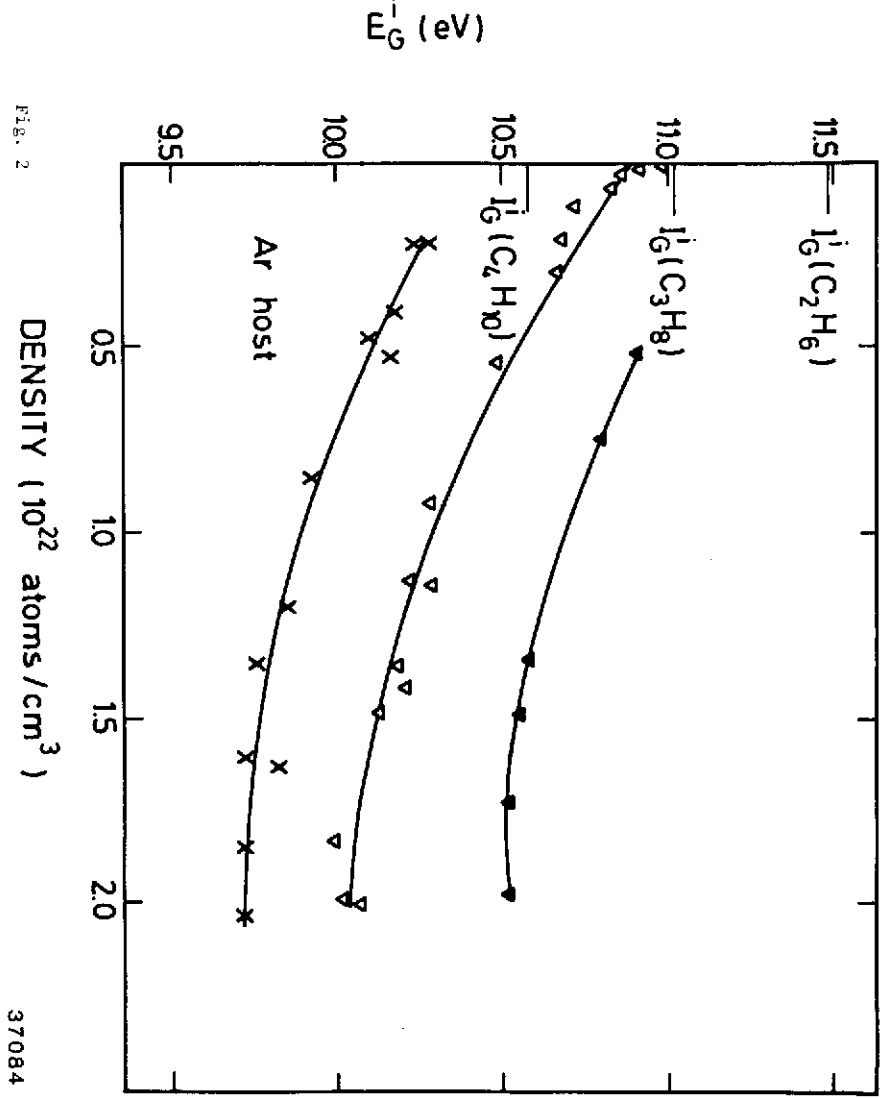
E_G^i (eV)
9.5
10.0
10.5
11.0
11.5
$I_G^i(C_2H_6)$
$I_G^i(C_3H_8)$
$I_G^i(C_4H_{10})$
Ar host
DENSITY (10^{22} atoms / cm^3)
0.5
1.0
1.5
2.0
37084

Fig. 2

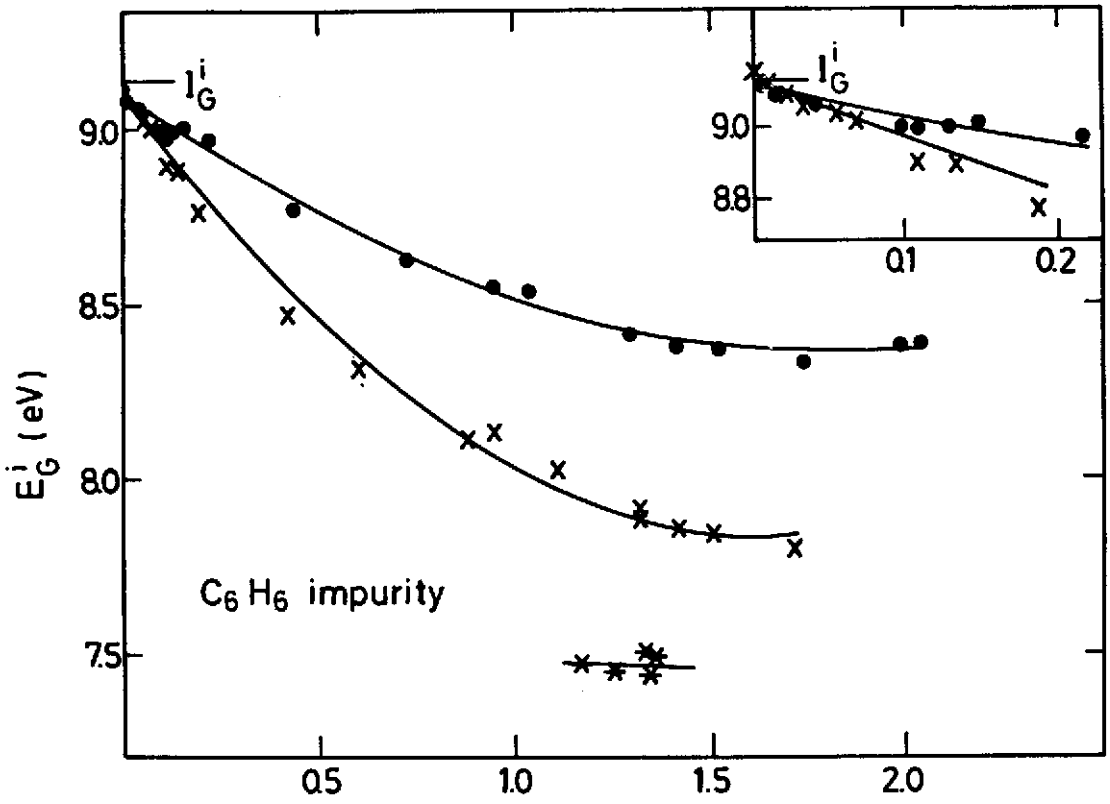

Fig. 3

37085

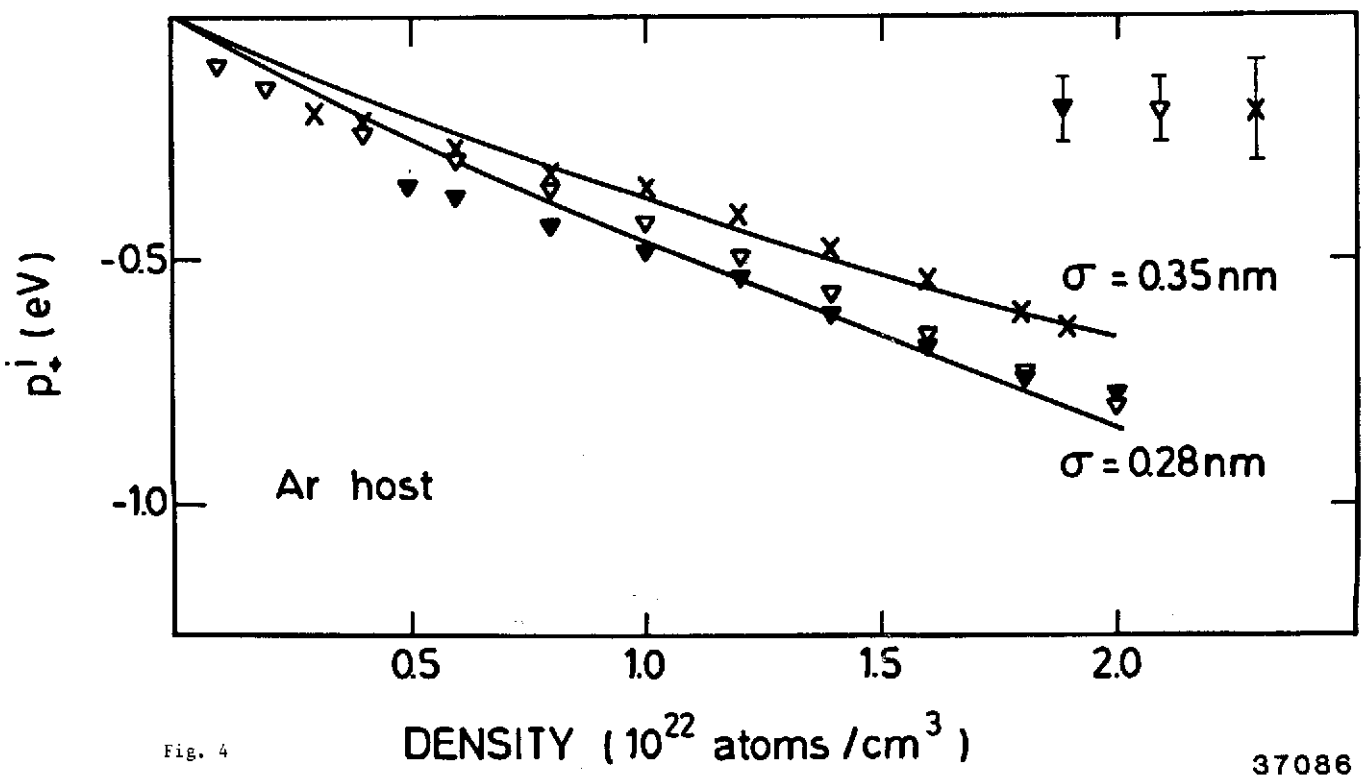

Fig. 4

37086

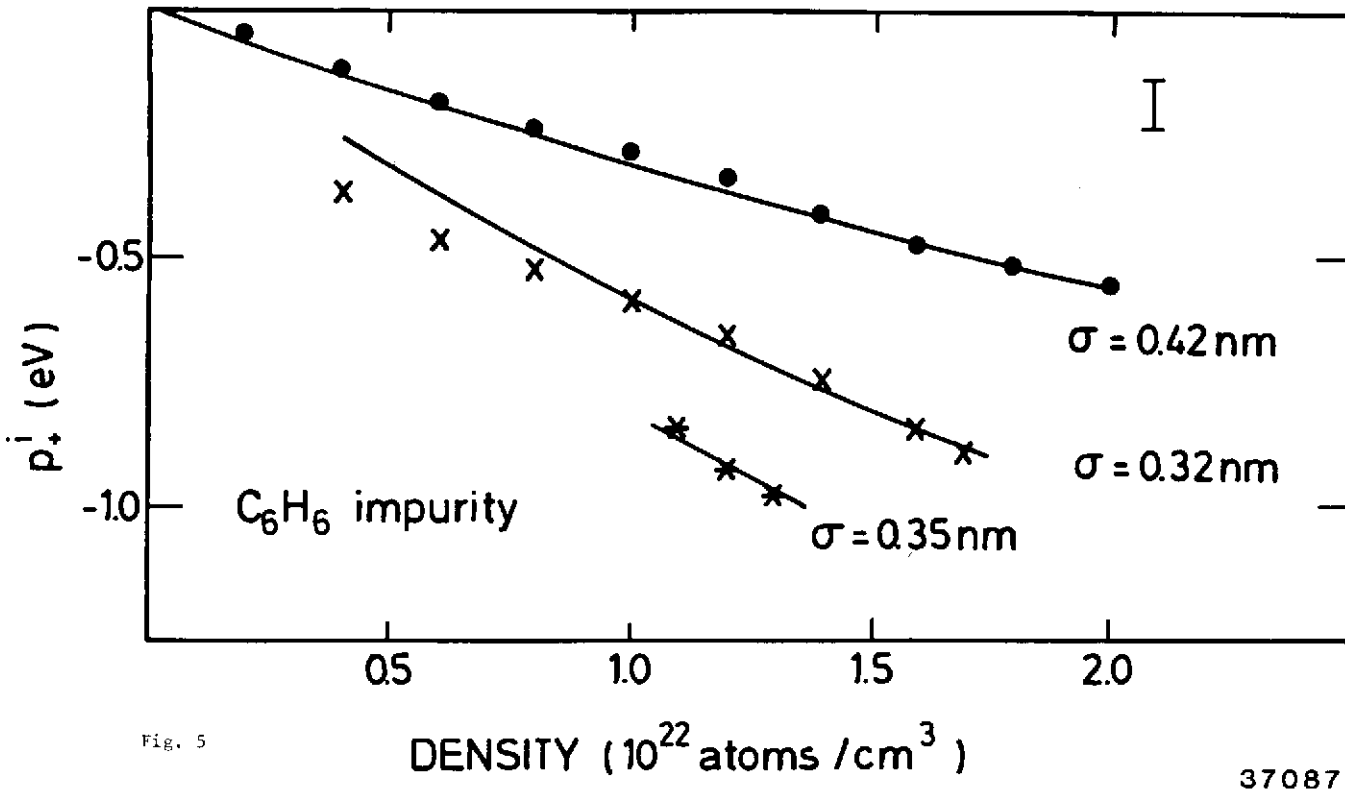
-0.5
-1.0
p_+^i (eV)
C_6H_6 impurity
σ = 0.42nm
σ = 0.32nm
σ = 0.35nm
0.5
1.0
1.5
2.0
DENSITY (10^{22} atoms / cm^3)
37087

Fig. 5